

A Molecular Mechanics Force Field for Alkylcobaloximes, a Model of Vitamin B₁₂ Coenzyme – Implications of Steric and Electronic Factors in the Co–C Bond Cleavage

Silvano Geremia,^[a] Mario Calligaris,^[a] and Lucio Randaccio*^[a]

Keywords: Cobaloximes / Vitamin B₁₂ / Semiempirical calculations / Force field / Conformation analysis / Cone angles / Crystal structure

Molecular mechanics force field constants have been derived for alkylcobaloximes, (alkyl)Co(DH)₂L (DH = monoanion of dimethylglyoxime and L = planar N-donor ligand), implementing the AMBER force field. Atomic charges have been calculated by the semiempirical ZINDO/1 method. Stretching and bending constants have been calculated by the Badger and Halgren equations, with the introduction of simple functions for the description of the electronic influence of the axial ligands on the coordination geometry. 26 parameters have been optimized, by the Simplex method, to fit 4523 bond lengths and angles of 52 alkylcobaloxime accurate crystal structures. In spite of the oversimplification of the adopted method for the description of the electronic effects, this approach provides a good description of the metal coordination geometries. The root-mean-square deviations of the calculated bond lengths and angles from the experimental values average to 0.023 Å and 1.4°, respectively. The molecular mechanics results are discussed in terms of the steric properties of the axial ligands and

correlated with their calculated cone angles. The force field has been used to analyse some conformational features of these compounds, such as the influence of the rotation of the axial ligands on their coordination geometry. The calculated energy for the Co–N rotational barrier agrees well with the experimental ones derived from dynamic and saturation ¹H-NMR spectroscopy in (alkyl)Co(DH)₂(2-NH₂-py). In order to have more experimental data for this analysis, the crystal structures of two new cobaloximes, (CH₂Cl)Co(DH)₂L with L = py, **1**, and 1-Me-Im, **2** have been determined. The results of a conformational analysis on ribosyl-imidazole derivatives, taken as a suitable vitamin B₁₂ coenzyme model, suggest that the 1-Me-imidazole-like ligands have a significantly greater rotation freedom with respect to the benzimidazole-like ones, but cause similar stretchings of the Co–C bond, and a significantly less stretching of the Co–N one. Implications for the recent findings on the binding mode of the coenzyme B₁₂ in the enzyme active site are discussed.

Introduction

For many years, simple organometallic octahedral Co^{III} complexes have been proposed as vitamin B₁₂ coenzyme models and a great amount of work on these systems has been performed in solution and in the solid state. Such extensive studies have provided a foundation for understanding the behaviour of the more complex vitamin B₁₂ system.^[1] The structurally accurate characterization of numerous complexes, RCo(chel)L, with several alkyl groups, R, and neutral Lewis bases, L, with chel = (DH)₂ (cobaloximes), (DO)(DOH)pn (Costa model), salen, saloph,^[2] has supplied an enormous amount of data,^[1b,1c,3] which has allowed in-depth analysis of the variations in geometry of the R–Co–L fragment, on the basis of the electronic and steric properties of the R and L groups^[4] as well as rationalization of the relationships between solution behaviour and structure.^[4–6]

It was deduced that, irrespective of the identity of the L and chel ligands (including corrin), the influence of R on the geometry of the R–Co–L fragment is evidenced by a

lengthening of the Co–L bond by up to 0.15 Å as the σ-donating ability of R increases (electronic *trans* influence) and by a lengthening of the Co–C bond by up to 0.20 Å as the bulk (steric *cis* influence) and the σ-donating ability of R increase.^[4b] Recently, a statistical analysis,^[4b] based on the Principal Component Analysis (PCA), of the variation with R of several experimental properties of alkylcobaloximes has suggested that the geometry of the axial fragment may be described fairly well by introducing three parameters, *t*₁, *t*₂, and *t*₃. Parameters *t*₁ and *t*₂ reflect the electronic and steric properties of R, respectively, whereas *t*₃ is related to the Co–CH₂–X angular deformation. It was found that the Co–C distances are a linear combination of the three parameters, whereas the axial Co–N distance is a linear function of only *t*₁.^[4b]

The influence of the bulk of L on the Co–L (steric *cis* influence) and on the Co–C (steric *trans* influence) distances has been structurally detected,^[7] the latter being particularly pronounced when R has a large bulk.^[8] Analogously, the Co–C bond dissociation energies (BDE) decrease with the increase in bulk of the phosphane in the two series RCo(DH)₂PR₃ when R = CH(Me)Ph and CH₂Ph.^[9] Structural evidence of the electronic influence of L on the Co–C bond is not so apparent.^[10] On the other hand, Halpern has found that the Co–C BDE increases with the increase of the p*K*_a of 4-substituted pyridines in the series

^[a] Dipartimento di Scienze Chimiche, Università di Trieste, I-34127 Trieste, Italy

Supporting information for this article is available on the WWW under <http://www.wiley-vch.de/home/eurjic> or from the author.

[CH(Me)Ph]Co(DH)₂(4-X-py).^[11] However, a large deviation from the BDE trend was detected when L = 2-NH₂-py,^[12a] due to the steric interaction of 2-NH₂-py with the equatorial moiety, which induces a lengthening of the axial Co–N bond by about 0.1 Å with respect to the analogous py derivative.^[12b] The Co–L bond is significantly influenced by the nature of chel (*cis* influence), while the Co–C bond is essentially unaffected,^[1c] although, very recently, it has been reported that the Co–C bonds in (DO)(DOH)pn complexes are slightly longer (0.01–0.03 Å) than in cobaloximes.^[6] Finally, it has been observed that the geometry of the Co(DH)₂ moiety is not affected by the nature of the axial ligands.^[1b,1c]

All these studies have given qualitative evidence of many properties of the Co coordination sphere in cobaloximes, which in many respects parallel those apparent in the vitamin B₁₂ system.^{[1][13]} Thus, as illustrated above, many chemical properties of cobaloximes and cobalamins, which are related to the metal coordination, involve steric influences. The first step in the catalytic cycle of the B₁₂-dependent isomerases is believed to be the homolytic cleavage of the Co–C bond and steric effects, acting in several ways, have been suggested to be responsible of the Co–C bond labilization.^{[13][14]} The task of quantifying steric interactions is not a simple one, although arguments invoking steric effects are intuitively appealing. Questions such as this should, in principle, be amenable to investigation by molecular mechanics (MM) methods, which have been proved to be a useful approach to investigate the structure and reactivity of coordination compounds.^[15–17] The combined application of X-ray crystallography and MM methods to the study of structural and conformational properties of metallo-organic systems represents a useful approach, and development and parametrization of suitable force fields are receiving increasing attention.^[18–21] Many reports which give force fields for Co^{III} compounds with N-donor ligands are available.^[16] However, only recently have force field parameters for cobalamins been proposed, based on the structures of six derivatives,^[19a] and for cobaloximes, on the basis of a large number of structures.^[19b] The last force field parameters for the Co–C bond and the Co–C–C angle have been transferred to the cobalamins, showing that the previously reached conclusions^[19a] remained essentially unchanged.^[19b] However, all these force fields, which we can call “conventional”, do not take into account the influence of electronic effects (e.g. *trans* influence) on the molecular geometry. An attempt to face this problem has been proposed by Rappé et al.,^[19c] with the introduction of empirical fractional bond orders, in their Universal Force Field (UFF). However, this correction is introduced a posteriori to improve the agreement between the calculated and the experimental distances. This approach does not allow reproduction of the observed continuous variation of the axial bond lengths when the bulk and the σ-donating ability of the axial ligands are varied, as it occurs in RCo(DH)₂L.^{[22][23]}

Recently, a new method for the optimization of force-field parameters, fitting experimental bond lengths and

angles, and using empirical functions for the calculation of stretching and bending constants, has been described.^[24] The present paper describes the derivation of force-field parameters for alkylcobaloximes, applying the above method, implemented with the introduction of a specific function, based on a fundamental parameter, which is assumed to take into account a priori the influence of the electronic factors on the coordination bond lengths and angles. Such an “unconventional” force field should permit the quantification of the intramolecular steric interactions contributing to the conformational properties. This should also allow a clear distinction of the origin (steric or electronic) of the observed structural deformations induced by the change of the axial ligands, such as the axial bond elongation, the orientation of the axial ligands with respect to the equatorial one and deformations in the equatorial moiety. In fact, there are many questions still open which are directly linked with the problem of the Co–C labilization.

The force-field parameters have been optimized to reproduce the X-ray structures of the 52 alkylcobaloximes, containing planar N-donor ligands, listed in Table 1. These include two new cobaloximes, (CH₂Cl)Co(DH)₂L, with L = py (**1**) and 1-MeIm (**2**), whose crystal structure have been determined in order to obtain further experimental data useful for the study of the influence of the orientation of L upon the Co–C and Co–N bond lengths. Finally, the biochemical implications of the MM calculations in the vitamin B₁₂ coenzyme model are discussed.

Results and Discussion

Methods

The AMBER force field^[25] has been selected, in view of its successful application to other coordination compounds,^{[17][24]} and the possibility of extension to the vitamin B₁₂ system. As known, in AMBER, the molecular strain energy, *E*, is given by the sum of deformation terms for bond lengths (*d*), bond angles (*θ*), and dihedral angles (*ψ*) (including improper torsion angles which model out-of-plane displacements), together with the van der Waals and electrostatic contributions:

$$E = \sum_b k^d (d - d^0)^2 + \sum_a k^\theta (\theta - \theta^0)^2 + \sum_d \{ V_n / 2 [1 + \cos(n\psi - \psi_0)] \} + \sum_{ij} (a_{ij}/r_{ij}^{12} - b_{ij}/r_{ij}^6 + q_i q_j / D r_{ij})$$

with $a_{ij} = (\epsilon_i \epsilon_j)^{1/2} (r_i^* + r_j^*)^{12}$ and $b_{ij} = 2(\epsilon_i \epsilon_j)^{1/2} (r_i^* + r_j^*)^6$, where r^* and ϵ are the van der Waals radii and the energy well depth, respectively, for two atoms of the same type, *q* is the atomic charge and *D* the dielectric constant.

Although the oxime bridge hydrogen atoms are found either symmetrically positioned between the oxygen atoms or bonded to one oxygen atom, we have assumed that the bridge hydrogen atoms are fixed to lie on the median of the O...O segment (Figure 1). The H atom is bonded to both O atoms in order to avoid large tetrahedral distortions of

Table 1. The axial ligands of the 52 RCo(DH)₂L complexes, whose structural data^[a] were used in the FF minimization; the solidus separates the two axial ligands R and L^[b]

1. adamantyl/1-Me-Im	27. NC(CH ₂) ₂ /3-Et-py	14. NC(CH ₂) ₃ /1,2-Me ₂ -Im	40. ClCH ₂ /1-Me-Im
2. adamantyl/1,5,6-Me ₃ -Bzm	28. NC(CH ₂) ₂ /3-Me-py	15. Me/1,2-Me ₂ -Im	41. ClCH ₂ /py
3. adamantyl/4-Me ₂ N-py	29. NC(CH ₂) ₂ /3-NC-py	16. Me/1-Me-Im	42. (NCCH ₂)(NC)CH/1,5,6-Me ₃ -Bzm
4. <i>c</i> -C ₆ H ₁₁ /1,5,6-Me ₃ -Bzm	30. PhCH ₂ /py	17. Me/Im	43. F ₃ CCH ₂ /4-NC-py
5. <i>i</i> Pr/1,2-Me ₂ -Im	31. (EtO ₂ C)(Me)CCH ₂ /py	18. Me/1,5,6-Me ₃ -Bzm	44. Cl(NC)CH/py
6. <i>i</i> Pr/1,5,6-Me ₃ -Bzm	32. NC(Me)CH/4-Me-py	19. Me/py	45. Cl ₂ CH/1,5,6-Me ₃ -Bzm
7. <i>i</i> Pr/py	33. NC(Me)CH/py	20. Me/6-Cl-purine	46. Cl ₂ CH/py
8. <i>i</i> Pr/2-NH ₂ -py	34. NC(Me)CH/4-NC-py	21. NC(CH ₂) ₂ /4-NH ₂ -py	47. O ₂ NCH ₂ /1,2-Me ₂ -Im
9. (Me ₃ C) ₃ CH ₂ /py	35. (MeO ₂ C)(Me)CH/py	22. NC(CH ₂) ₂ /1-Me-Im	48. O ₂ NCH ₂ /1,5,6-Me ₃ -Bzm
10. Et/4-[(MeO)C=NH]-py	36. (MeO ₂ C)(Me)CH/4-Cl-py	23. NC(CH ₂) ₂ /4-Et-py	49. O ₂ NCH ₂ /py
11. Et/1,5,6-Me ₃ -Bzm	37. (MeO ₂ C)(Me)CH/4-NC-py	24. NC(CH ₂) ₂ /4-Me-py	50. F ₃ C/py
12. Et/py	38. NCCH ₂ /1,2-Me ₂ -Im	25. NC(CH ₂) ₂ /py	51. Cl ₂ (NC)C/1,2-Me ₂ -Im
13. ribosyl ^[c] /py	39. NCCH ₂ /py	26. NC(CH ₂) ₂ /3-NH ₂ -py	52. (F ₃ C) ₃ CF/py

^[a] Structural data are taken from the Cambridge Structural Data Files, except those of 40 (1) and 41 (2) reported in the present work.

– ^[b] Im = imidazole, Bzm = benzimidazole. – ^[c] ribosyl = 5-deoxy-β-D-ribofuranos-5-yl.

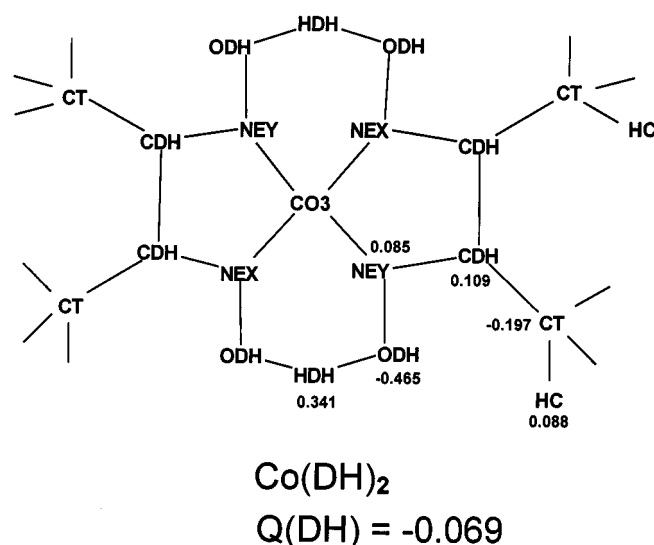


Figure 1. Atom types and charges for the equatorial Co(DH)₂ moiety

the equatorial moiety. Atom types are given in Figures 1 and the Supporting Information.

Energy calculations have been performed with a Pentium-200 PC, using the HYPERCHEM 4.5 molecular modeling package.^[26] The Polak–Ribiere version of the conjugate gradient method was used in all energy minimizations, until the convergence criterion of 0.001 kcal mol⁻¹ Å⁻¹ was reached.

As previously reported,^[24] the potential constants for all *i*–*j* bonds were calculated from Badger's rule,^[27] $k_{ij}^d = [(A_{ij} - D_{ij})/(d_{ij}^0 - D_{ij})]^3$, using the parameters proposed by Herschbach and Laurie,^[28] while potential constants for the *i*–*j*–*k* bond angles were calculated from the Halgren's equation:^[29] $k_{ijk}^0 = 1.75 Z_i C_j Z_k (d_{ij} + d_{ik})^{-1} (\theta_{ijk}^0)^{-2} \exp[-2(d_{ij} - d_{jk})^2/(d_{ij} + d_{ik})^2]$. This approach allows automatic variation of the stretching and bending constants as a function of the reference bond lengths (d_{ij}^0) and angles (θ_{ijk}^0). For cobalt, two different *C* values (*cis* and *trans* bonds) and one *Z* value were assumed. Force-field constants, reported in Table 2, were optimized by an iterative procedure, in which the sum of the squares of the differences (Δ) between observed and calculated values were re-

duced upon variation of the parameters.^[30] The observables are the bond lengths and angles of 52 accurate (crystallographic *R* index < 0.08) crystal structures of alkylcobaloximes (Table 1). Weights were assigned to the experimental data on the basis of the average estimated errors, $w = 1/\sigma^2$. Since several of the starting structures were taken from CSD (version 1997), where individual errors for bond lengths and angles are not reported, these were evaluated for each structure from the average differences among chemically equivalent parameters of the Co(DH)₂ moiety, $\bar{\sigma}$. In order to take into account the different accuracy in the atom location, related to the different electron density, the $\bar{\sigma}$ values were weighted on the basis of the atomic numbers *Z*, according to the equation $\sigma_w = [\Sigma(\bar{\sigma} \cdot Z \cdot n)]/\Sigma n$, where *Z* is the sum of atomic numbers of the atoms involved in the bond length or angle and *n* is the number of chemically equivalent parameters. In this calculation summations were extended over the different types of bond lengths or bond angles. The two σ_w values, for distances and angles, respectively, were used to calculate individual estimated errors as $\sigma = \sigma_w/Z$. The σ values obtained by this procedure well agree with the available experimental values, therefore providing a useful way to evaluate σ values for CSD data.

As for the previously reported Ru–sulfoxide complexes,^[24] the optimization procedure was performed by adopting the Simplex method, in view of the non-linear nature of the equations and the facility of introducing restraints in the minimization.^[31] Convergence was controlled by a goodness-of-fit (GOF) parameter defined as $[\Sigma w \Delta^2/(n_{\text{obs}} - n_p)]^{1/2}$, where *n*_{obs} = number of observables and *n*_p = number of parameters. Convergence was reached when the absolute relative difference between the lowest and the highest GOF values was less than 0.0001. During the preliminary refinement a marked discrepancy between the observed and calculated axial Co–N distance was found for the 2-NH₂-py derivative, together with relatively high differences between the axial Co–N–C bond angles. Change of the aminic group hydrogen atom type from H to H1 yielded a remarkable improvement, so that H1 was taken as the atom type for hydrogen atoms attached to nitrogen atoms. Torsional barriers around C–C and C–N bonds were calcu-

Table 2. Optimized force field constants (a [Å], b [Å/e], C , Z , ϵ [kcal mol⁻¹], r^* [Å], d^0 [Å], θ^0 [°], D), and related stretching and bending constants (k^d [kcal mol⁻¹ Å⁻²], k^0 [kcal mol⁻¹ rad⁻²])

$a_{\text{Co-C}}$	1.959	
$b_{\text{Co-C}}$	0.17	
$a_{\text{Co-N}}$	1.997	
$b_{\text{Co-N}}$	0.30	
$C_{\text{CO}_3^{[a]}}$	0.52	
$C_{\text{CO}_3^{[b]}}$	3.23	
Z_{CO_3}	1.15	
ϵ_{CO_3}	0.502	
$r_{\text{CO}_3}^*$	1.691	
D	7.8	
Stretching constants		
	k^d	d^0
CO ₃ -NER ^[c]	94.9	1.997
CDH-CDH	325.1	1.424
CDH-NER ^[c]	607.5	1.284
ODH-NER ^[c]	457.3	1.344
ODH-HDH	198.9	1.269
Bending constants		
	k^0	θ^0
CO ₃ -NER-ODH ^[c]	61.6	123.8
CO ₃ -NER-CDH ^[c]	48.5	124.6
CDH-CDH-NER ^[c]	76.4	117.8
CT-CDH-NER ^[c]	70.8	120.2
CO ₃ -NAZ-C ^[d]	50.6	122.0
CO ₃ -CAZ-F	61.4	110.6
CO ₃ -CAZ-C ^[c]	55.4	111.7
CO ₃ -CAZ-CL	60.4	111.6
CO ₃ -CAZ-N	63.7	108.3
CL-CAZ-CL	74.3	110.1
F-CAZ-F	97.8	102.9

[a] For $\theta^0 = 90^\circ$. - [b] For $\theta^0 = 180^\circ$. - [c] $R = \text{X}, \text{Y}$. - [d] $C = \text{CA}, \text{CK}, \text{CQ}$; $k^0 = 50.4$ for CB and 50.5 for CW. - [e] $C = \text{C}, \text{CT}$; $k^0 = 55.5$ for CA and 55.7 for C1.

lated as in AMBER.^[25] Barriers around coordination bonds were not considered.^[32]

The observed bond lengths and, particularly, the coordination bond angles can be slightly modified by packing effects, which can force the molecule into a strained conformation. In order to simulate crystal packing effects, the torsional angles around single bonds and involving non-H atoms were constrained by a 16 kcal mol⁻¹ energy barrier in the energy minimization to maintain the crystal structure conformation.

For the electrostatic contribution, atomic charges were calculated by the semi-empirical ZINDO/1 method, included in HYPERCHEM 4.5.^[26] Charges of chemically equivalent atoms were averaged over the same ligands. The cobalt atom charges assured the electroneutrality of the complexes. Atom types and charges for the Co(DH)₂ moiety are shown in Figure 1, while for the R and L groups they are given in the Supporting Information, together with total charges, Q . The *vacuum* value ($D = 1$) was initially assumed for the dielectric constant. However, this value was refined since the inclusion of the dielectric constant in the optimization process ensures the proper scaling of the electrostatic contribution. The final value of 7.8 is consistent with the fact that we are considering solid-state and not gas-phase structures.

Since the Co-C and Co-N axial bonds are significantly influenced by the electronic nature of R,^{[1][4]} the force-field

parameter optimization procedure was carried out in two steps. In the first step, electronic effects were neglected, thereby producing approximate parameters for the functions involving the equatorial ligand atoms, together with "average" d^0 values for the axial Co-C and Co-N bonds. At convergence ($d_{\text{Co-C}}^0 = 1.964$, $d_{\text{Co-N}}^0 = 2.007$ Å), the goodness of fit was quite reasonable: GOF = 3.48 for 4523 observables and 24 variables. However, as expected, the differences between observed and calculated Co-C and Co-N axial distances were rather high (see Table 3). In fact, in this step (constant d^0 values for Co-C and Co-N distances) the calculated axial distances can only reflect the steric contribution and not the electronic one. Thus, the differences (δ) between the calculated and observed axial distances should be related to the σ -donating ability of the R group. As a measure of the latter, the total electrostatic charge of R, Q , was taken. The validity of this choice is supported by the fairly good linear relationship ($r = 0.91$, $n = 21$) between Q and the available values of EP, which have previously been shown to provide an experimental measure of the electron-donating ability of R.^[4a] In fact, the δ values for the Co-C and Co-N distances correlate well with Q , the correlation coefficients being 0.83 and 0.94, respectively.

Table 3. Average differences, $\langle\Delta\rangle$, between observed and calculated bond lengths [Å] and angles [°], together with rms values and number of observations, n , after the first and second step of the force field parameter optimization process; X, Y, Z represent generic non-metal atoms

Distances	n	first step $\langle\Delta\rangle$	rms	second step $\langle\Delta\rangle$	rms
Co-N equatorial	208	0.004	0.010	0.004	0.009
Co-N axial	52	-0.014	0.028	0.008	0.016
Co-C axial	52	-0.016	0.032	-0.003	0.020
X-Y equatorial	728	-0.009	0.017	-0.008	0.017
X-Y axial	592	-0.016	0.031	-0.016	0.031
All distances	1632	-0.010	0.024	-0.009	0.023
Angles					
Co-N-X equatorial	416	-0.1	0.6	-0.1	0.6
Co-C(N)-X axial	177	0.1	1.8	-0.1	1.8
X-Co-Y	780	-0.2	1.4	-0.2	1.3
All angles	2891	-0.1	1.4	-0.1	1.4

In order to take into account the different electronic effect of the R groups on the Co-C and Co-N axial distances,^{[1][4]} in the second optimization step, the d^0 values of the Co-C and Co-N bonds were assumed to be a linear function of Q , according to Equations 1 and 2.

$$d_{\text{Co-C}}^0 = a_{\text{Co-C}} + b_{\text{Co-C}}Q \quad (1)$$

$$d_{\text{Co-N}}^0 = a_{\text{Co-N}} + b_{\text{Co-N}}Q \quad (2)$$

The coefficients of Equations 1 and 2 were optimized, together with all the other force-field parameters. At convergence, the GOF value reduced to 3.30 for $n_{\text{obs}} = 4523$ and $n_p = 26$.

Final values of the refined parameters are reported in Table 2, together with the calculated stretching and bending

constants. All force-field constants are reported in the Supporting Information.

The potential energy for the isolated molecules ($D = 7.8$) were explored using local Excel© Macro functions, which allow the minimization of the strain energy as the conformation of the molecule is varied through rotation around the axial Co–N bond, ψ . The torsional angle was varied in 5° steps from -180° to 180° , introducing a constraint of $1000 \text{ kcal mol}^{-1}$. The zero value of ψ was taken at the point where the plane of L bisects the oxime bridge. The minimum energy conformer was finally minimized using a convergence gradient of $0.001 \text{ kcal mol}^{-1} \text{ \AA}^{-1}$.

Cone angles for the axial ligands were calculated according to the Immirzi's algorithm,^[33] as modified in ref.^[21], using the atom coordinates of the 52 energy minimized structures. The van der Waals radii used for the ligand atoms were those given by Bondi,^[34] assigning a zero value to the metal-coordinated atoms. The solid cone angle Ω and the corresponding Tolman's angle Θ were calculated at distances corresponding to the Co–C and Co–N d° values of Equations 1 and 2 and averaged for each axial ligand. The Ω and Θ values are given in Table 4 together with the $d^\circ(\text{R})$ and $d^\circ(\text{L})$ values.

X-ray Diffraction Analysis of Compounds 1 and 2

The ORTEP drawings with the atom numbering scheme for **1** and **2** are given in Figures 2 and 3, respectively. The schemes apply to both the crystallographically independent molecules A and B. The molecules A and B of **1** are very similar, while in **2** they display different orientations of both the axial groups with respect to the equatorial ligand, which cause a slight, but significant, difference in the Co–N axial distance and in the Co–C–Cl bond angles. In **1** the torsional angles around the Co–N(py) bond (ψ) and the

Co–C bond (ϕ) are 4° and 74° in A, and 3° and 72° in B, respectively. On the other hand, in **2** the corresponding angles are 49° and -47° in A, and 38° and -105° in B.

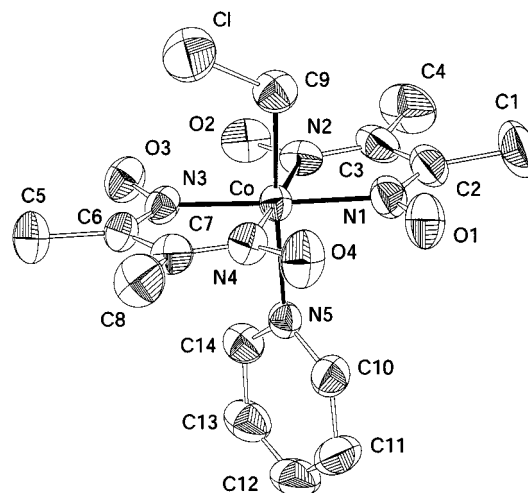


Figure 2. ORTEP drawing (50% thermal ellipsoids) of **1** together with the atom numbering scheme

It is of interest to compare the 1-Me-Im orientation in A and B with those found in other derivatives with $\text{R} = \text{Me}$, $\text{CH}_2\text{CH}_2\text{CN}$, and adamantyl. In the last derivative, the 1-Me-Im plane nearly bisects the oxime bridge ($\psi \approx 0^\circ$), whereas in the others it approximately crosses the equatorial five-membered rings ($\psi \approx 90^\circ$).^[1c] This comparison indicates that there is significant conformational freedom for rotation around the Co–N(1-Me-Im) bond when R has a relatively small bulk. Conversely, the rotation is hindered in the case of very bulky R groups such as adamantyl, which imposes the bending of the equatorial moiety towards the *trans* N ligand and, consequently, forces the latter into the orientation with $\psi \approx 0^\circ$. Such confor-

Table 4. $d^\circ(\text{R})$ [\AA], $d^\circ(\text{L})$ [\AA], Ω [ster rad] and Θ [$^\circ$] values for R and L ligands

R	$d^\circ(\text{R})$	$d^\circ(\text{L})$	Ω	Θ	L	Ω	Θ
Me	1.960	1.999	1.85	90.3	Im	1.99	93.9
CH_2Cl	1.943	1.969	2.18	98.4	1-Me-Im	1.99	93.9
NCCH_2	1.944	1.970	2.21	99.2	py	2.24	100.0
Et	1.966	2.010	2.29	101.0	1,5,6-Me ₃ -Bzm	2.28	100.8
$\text{NC}(\text{CH}_2)_3$	1.961	2.001	2.30	101.3	1,2-Me ₂ Im	2.40	103.8
F_3C	1.924	1.936	2.33	102.0	6-Cl-purine	2.68	110.0
O_2NCH_2	1.925	1.937	2.38	103.3	2-NH ₂ -py	2.87	114.2
$\text{NC}(\text{CH}_2)_2$	1.958	1.996	2.41	103.8			
Cl_2CH	1.927	1.940	2.52	106.5			
F_3CCH_2	1.938	1.960	2.53	106.7			
$\text{Cl}(\text{NO})\text{CH}$	1.931	1.948	2.55	107.1			
PhCH_2	1.957	1.993	2.61	108.4			
$\text{NC}(\text{Me})\text{CH}$	1.951	1.984	2.66	109.6			
$(\text{NCCH}_2)(\text{NC})\text{CH}$	1.942	1.967	2.67	109.9			
ribosyl	1.963	2.003	2.69	110.3			
<i>i</i> Pr	1.971	2.017	2.75	111.5			
<i>c</i> -C ₆ H ₁₁	1.972	2.020	2.79	112.4			
$(\text{MeO}_2\text{C})(\text{Me})\text{CH}$	1.947	1.975	2.88	114.3			
$\text{Cl}_2(\text{NC})\text{C}$	1.911	1.913	2.90	114.8			
$(\text{Me}_3\text{C})_3\text{CH}_2$	1.968	2.013	3.00	116.9			
$(\text{EtO}_2\text{C})_2(\text{Me})\text{CCH}_2$	1.956	1.991	3.31	123.4			
adamantyl	1.975	2.026	3.32	123.7			
$(\text{F}_3\text{C})_3\text{CF}$	1.906	1.903	3.49	127.2			

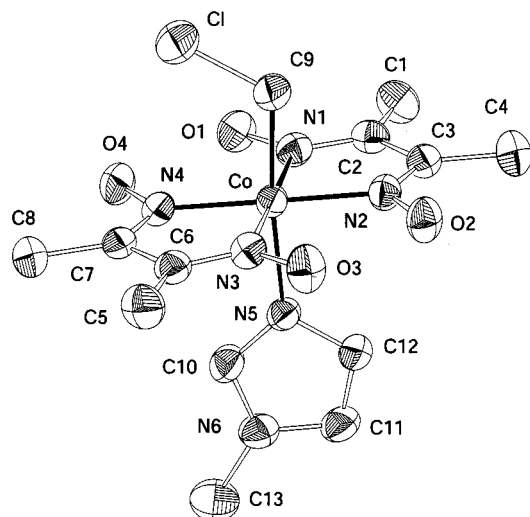


Figure 3. ORTEP drawing (50% thermal ellipsoids) of **2** together with the atom numbering scheme

mational freedom is typical of Im and 1-Me-Im ligands, since in all the structurally characterized alkylcobaloximes containing planar N ligands – such as 1,5,6-Me₃-Bzm, 1,2-Me₂-Im and py – only the orientation with $\psi \approx 0^\circ$ is found, regardless of the bulk of the R group.^[1c]

Validation of the Force Field

The consistency of the force field can be evaluated from the average values of the differences ($\langle\Delta\rangle$) between observed and calculated bond lengths and angles and their root-mean-square deviations, $\text{rms} = [(\sum\Delta^2)/n]^{1/2}$. Deviation from zero of the average values gives a measure of the asymmetry of the Δ distribution or indicates the presence of systematic errors, while rms gives a measure of the spread of the Δ values and hence of the fit between calculated and experimental structures. The agreement between observed and calculated values appears to be quite satisfactory, especially after the second optimization step, as shown in Table 3. Inspection of Table 3 reveals a marked reduction of both the $\langle\Delta\rangle$ and rms values after the second parameter optimization step only for the axial Co–C and Co–N distances, while for the other bond lengths and angles no significant improvement in $\langle\Delta\rangle$ and rms values is apparent. In fact, only the axial distances are strongly affected by electronic factors, which are not taken into account in the model used in the first step. This improvement supports the assumption that the electronic factors, introduced in the second optimization step, are related to the overall charge Q of the alkyl group according to Equations 1 and 2. The axial Co–C and Co–N distances are fairly well reproduced, as shown in Figure 4, where the observed values are plotted against those calculated for the 52 cobaloximes.

In order to evidence the improvement on the axial distances derived from the introduction of the electronic factor, the experimental values are compared in Table 5 with those calculated after the first and the second step, for the

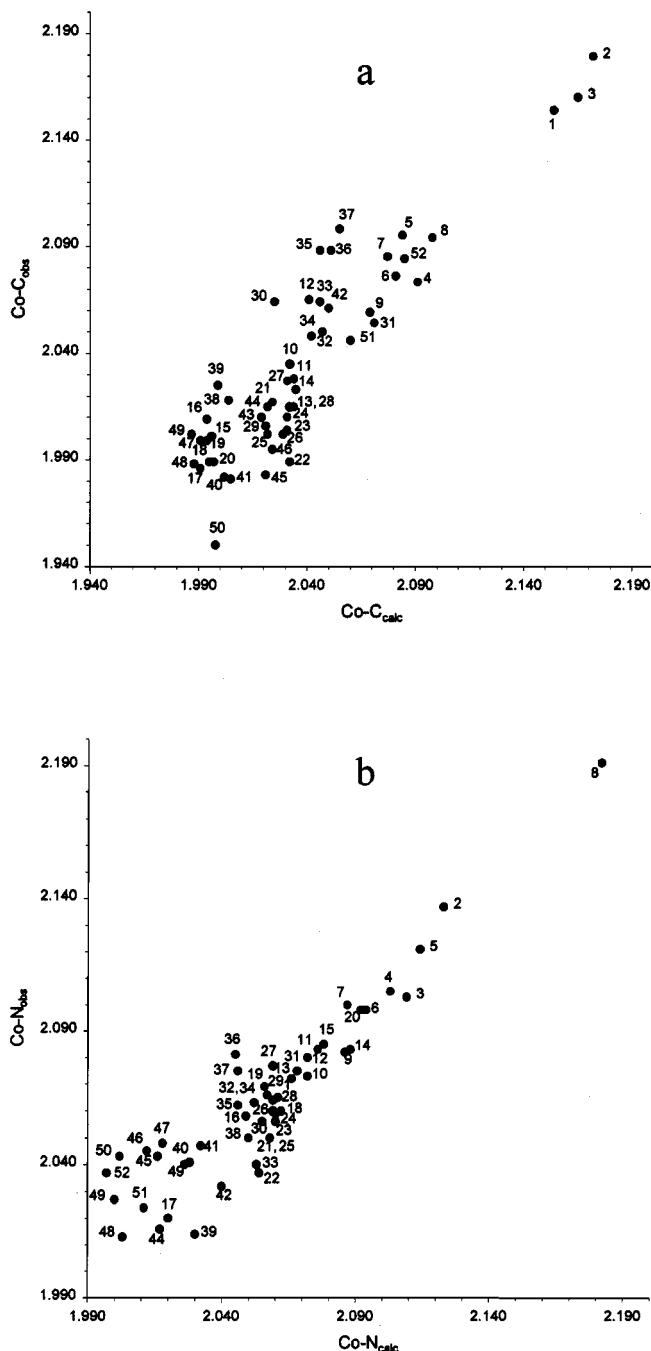


Figure 4. Plot of the observed vs. calculated Co–C (a) and Co–N (b) axial distances

series $\text{RCo}(\text{DH})_2(1,2\text{-Me}_2\text{Im})$, having R with significantly different bulk and σ -donating ability and a relatively bulky N-donor ligand. It is also apparent that the introduction of the electronic factor well reproduces the shortening of both the Co–C and Co–N bonds when R is an electron-withdrawing group such as CCl_2CN , in agreement with the PCA results.^[4b]

The geometry of the Co–R grouping is characterized by experimental Co–C(sp³)–X angles which span a rather wide range, from 113.7° to 130.3° , and increase with the increasing of the bulk of X. This variation is well repro-

Table 5. Observed and calculated Co–C and Co–N bond lengths [Å] for RCo(DH)₂(1,2-Me₂Im), after the first and second step of the present force field parameter optimization process

R		obs	step 2	step 1
CCl ₂ CN	Co–C	2.046	2.060	2.115
	Co–N	2.024	2.011	2.108
CH ₂ NO ₂	Co–C	1.999	1.991	2.030
	Co–N	2.048	2.018	2.090
CH ₂ CN	Co–C	2.018	2.004	2.031
	Co–N	2.050	2.050	2.090
CH ₂ CH ₂ CN	Co–C	2.023	2.035	2.038
	Co–N	2.083	2.088	2.094
Me	Co–C	2.001	1.996	1.999
	Co–N	2.085	2.078	2.086
<i>i</i> Pr	Co–C	2.095	2.084	2.079
	Co–N	2.121	2.114	2.103

duced by the present force field, with just a few exceptions (see below). However, the differences between observed and calculated values appear quite acceptable if we consider that experimental values may be affected by several errors. For example, diffraction data quality (crystal quality), thermal motion effects or local static disorder, and residual packing and electronic effects.^[25] In fact, for only two out of the nine (NCCH₂CH₂)Co(DH)₂L derivatives considered are large differences between the observed and calculated Co–C–C angle detected when L = py^[4a] (6.5°) and 1-Me-Im^[35] (11.2°), whereas for the other derivatives the differences do not exceed 1.9°. The two structures were accurately refined to *R* = 0.042,^[4a,35] but inspection of atomic parameters shows that the thermal B factors of the C-β atom in both cases are anomalously high (by about a factor of three) relative to those of the other atoms, indicating a significant statistical occupancy disorder of that atom. Finally, the largest disagreement in the axial bond lengths is observed in the complexes containing COOMe and halogens bonded to the C-α atom (Figure 4).

Besides the general agreement between the observed and calculated structures, the validity of the present force field is further illustrated by its ability to reproduce the angular deformations around the metal center (Table 3), even using the same unstrained values of 90° or 180° for metal coordination angles. In particular, the experimental values for the equatorial N–Co–N angles average to 98.7° on the side of the oxime bridge and to 81.3° on the other side. The calculated values average to 98.5° and 81.5°, respectively. Furthermore, the remarkable angular deformations of the two Co–N(sp²)–C angles for the coordinated lopsided ligands 1,5,6-Me₃-Bzm, 1,2-Me₂-Im, 2-NH₂-py, and 6-Cl-purine are very well reproduced, even using the same unstrained value for all the Co–N–C angles (122.0°). In fact, in these derivatives, the experimental values of the two angles differ significantly, with average values of 133.5/120.7°, 133.4/121.6°, 129.7/115.6°, and 125.9/120.6°, respectively, whereas the corresponding calculated values are 132.9/121.8°, 131.5/122.8°, 125.5/117.2°, and 125.2/120.2°.

Finally, it is of interest to compare the results of this force field for (CN)(CH₂CN)CHCo(DH)₂(1,5,6-Me₃Bzm) with

those obtained by UFF^[19c] for the same structure (Table 6). The Δ differences between observed and calculated values are similar for the Co–C distance, while the Co–N bond length, which undergoes a strong *trans* influence, is much better reproduced by the present force field.

Table 6. Differences, Δ [Å], between observed and calculated Co–C, Co–N(ax), and Co–N(eq) bond lengths for (EtO₂C)₂-(Me)CCH₂Co(DH)₂(py), obtained after the first and second step of the present force field parameter optimization process and after UFF calculations

Δ	step 1	step 2	UFF
Co–C	–0.027	–0.017	–0.023
Co–N(ax)	0.009	0.006	0.047 ^[a]
Co–N(eq)	0.002	0.006	–0.043

[a] Assumed bond order, 1/2.

Cone Angles

According to the proposed model, the difference, δ, between the observed Co–L and Co–R axial distances and the corresponding *d*^p(Co–R) and *d*^p(Co–L) values should give the lengthening due to steric effects. Therefore, the δ values were expected to correlate with the bulkiness of the axial ligands, as measured by their cone angles. In fact, as shown in Figure 5, fairly good linear relationships are found, supporting the hypothesis that the steric and electronic contribution to the bond length can be considered approximately additive.

Conformational Analysis

For MeCo(DH)₂L derivatives (L = Im, py, 1,5,6-Me₃-Bzm, 1,2-Me₂-Im, 6-Cl-purine, and 2-NH₂-py) the variation of the strain energy with ψ, scaled to its minimum value, is shown in Figure 6a in the range from –180° to +180°. All the curves have similar shapes with the lowest minimum at ψ = 0° and a rather broad, but structured, higher energy region around ψ = 90° ± 32°, which is particularly apparent for lopsided ligands. The latter region is characterized by two maxima and one minimum in between, with small energy differences (< 1.5 kcal mol^{–1}), for all the ligands, except 2-NH₂-py, where three maxima and two minima are observed (Figure 6a). However, the rotational energy barrier, *E*_{rot}, significantly increases from L = Im (*E*_{rot} ≈ 2 kcal mol^{–1}), to L = py, 1,2-Im, 1,5,6-Me₃-Bzm (*E*_{rot} ≈ 4 kcal mol^{–1}) up to L = 2-NH₂-py (*E*_{rot} ≈ 10 kcal mol^{–1}). The variation in the axial Co–N distance with ψ, given in Figure 6b, follows a similar trend, showing that the shortest distances occur at ψ = 0° and the longest ones around ψ = 90°, for all the L ligands, with differences, Δ*d*, which increase from L = Im (Δ*d* = 0.02 Å), to L = 2-NH₂-py (Δ*d* = 0.05 Å).

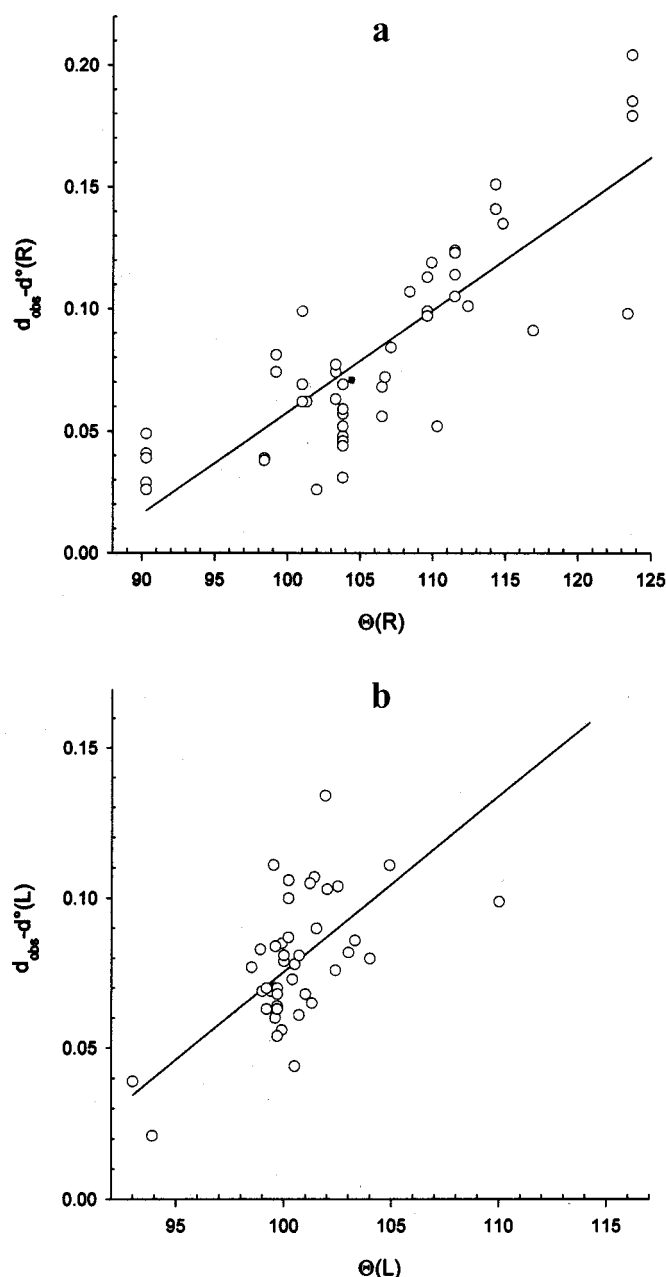


Figure 5. Plot of the differences $d(\text{obs})_{\text{Co-R}} - d^0(\text{R})$ (a) and $d(\text{obs})_{\text{Co-L}} - d^0(\text{L})$ (b) vs. Tolman's cone angles $\Theta(\text{R})$ and $\Theta(\text{L})$, respectively

Axial Co–N Distances

The fairly linear trend between the $d^0(\text{Co-N})$ values and the experimental axial distances in complexes with the same L ligand suggests that these distances are essentially influenced by the σ -donating ability of the R groups. However, the present calculations indicate that the bulk (Figure 5b) and the orientation (Figure 6b) of the planar L ligand influence the axial Co–L bond length, as previously suggested.^[1b] Since in the present model the electronic influence of R on the Co–L distance is taken into account by $d^0(\text{Co-L})$, the difference between the experimental values and d^0 , $\delta(\text{Co-L}) = d(\text{Co-L}) - d^0(\text{Co-L})$, should re-

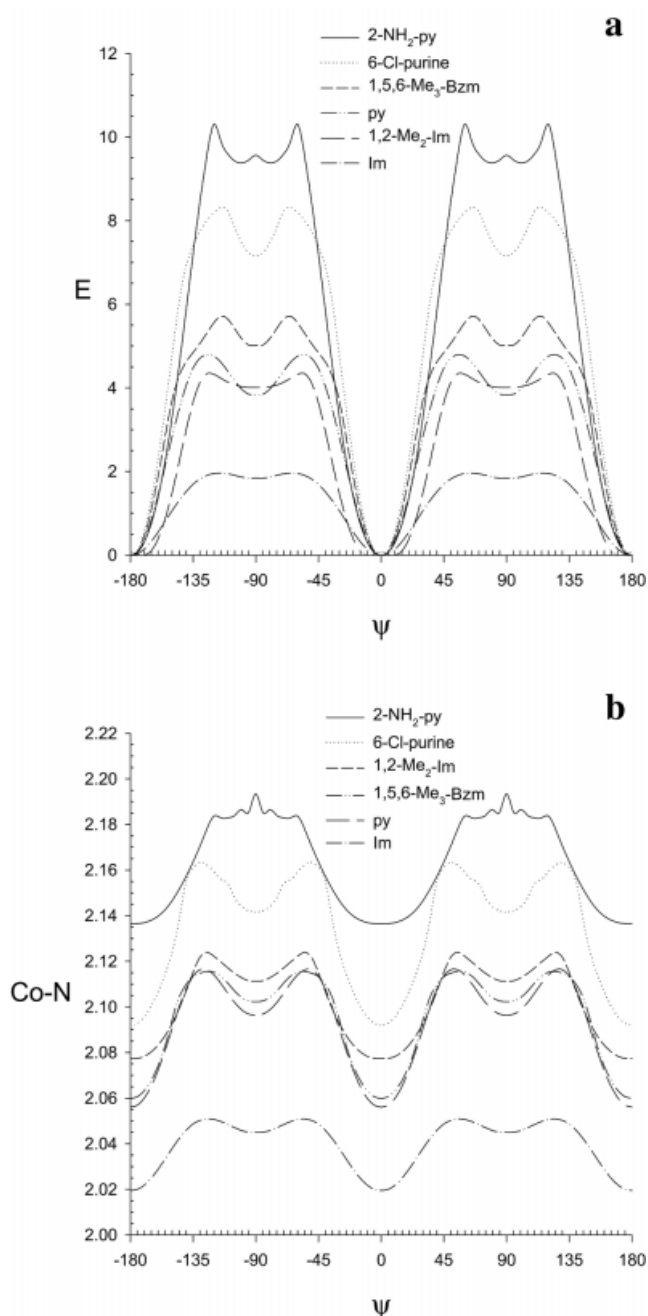


Figure 6. Plot of the strain energy (a) and of the Co–N axial distance (b) vs. ψ for different L ligands

present the contribution to the distance ascribable to the bulk and orientation effects. Within this assumption, $\delta(\text{Co-L})$ should correlate with the calculated cone angles of the L ligands, $\Theta(\text{L})$, having the same orientation. In fact, a good correlation is found, as shown in Figure 5b for all the cobaloximes in which the L orientation nearly corresponds to $\psi \approx 0^\circ$, i.e. in all the examined cobaloximes, with the exclusion of most of those having L = 1-Me-Im or Im. The vertical spread in Figure 5b could be related to the steric *trans* influence on the Co–L bond due to the R groups, which are able to induce an appreciable bending of the equatorial moiety towards L, displacing the latter and

lengthening the *trans* Co–L bond.^[7] Thus, when L = 1,5,6-Me₃-Bzm, $\delta(\text{Co}–\text{N})$ is 0.061 Å for R = Me and 0.111 Å for R = adamantyl, and the bending angles between the two DH units are 4.7° and –6.1°, respectively (the negative sign indicates bending towards L). The energy profiles, reported in Figure 6a for the different L ligands, clearly show that the rotation around the Co–N axial bond is significantly less hindered when L = Im, where the rotational barrier is about 2 kcal mol^{–1}, while this increases to 4 and 10 kcal mol^{–1} going from py to 2-NH₂-py. This is the reason why only for cobaloximes containing the Im (or 1-Me-Im) ligand are different orientations of L observed in the crystal, as evidenced above in the section Description and Discussion of the Structures. In fact, in RCo(DH)₂(1-Me-Im), $\psi = 66^\circ$ when R = Me, $\psi = 67^\circ$ when R = CH₂CH₂CN, and $\psi = 38$ and 49° when R = CH₂Cl. It is very likely that in these structures crystal forces are strong enough to stabilize different orientations, overwhelming the rotation energy barriers. Conversely, with the other L ligands having higher torsional barriers only the orientation with $\psi \approx 0^\circ$ is found in the solid state.^[1b] Inspection of Figure 6b, in which the trend of the Co–N distance vs. ψ is shown, indicates also that the lengthening of the latter distance increases significantly for the same non-zero ψ value in the order Im \approx 1-Me-Im < py \approx 1,5,6-Me₃Bzm \approx 1,2-Me-Im < 6-Cl-purine < 2-NH₂-py. Finally, it is worthwhile noting that for L = 2-NH₂-py, the barrier height between $\psi = 0^\circ$ and $\psi = 90^\circ$ is about 10 kcal mol^{–1}, a value very close to the activation energies (9.2–13.1 kcal mol^{–1}) for rotation about the axial Co–N bond as derived from dynamic and saturation ¹H-NMR spectroscopy for the RCo(DH)₂(2-NH₂-py) complexes [R = *i*Pr, Et, neopentyl, CH₂Br, CH₂C(Me)(CO₂Et)₂, CH₂CN, and CH₂NO₂].^[36] The two limit orientations, $\psi = 0^\circ$ and $\psi = 90^\circ$, are generally distinguished as A and B, respectively.^[1c,6,23] These observations lead to the suggestion that the L orientation is principally determined by steric factors (crystal packing forces in 1-Me-Im derivatives, and intramolecular forces in the other L-containing derivatives) more than to electronic ones.^[1c,3a,36]

Axial Co–C Distances

Unlike the Co–N distances, the experimental Co–C distances do not correlate with the $d^p(\text{Co}–\text{C})$ values and, therefore, are significantly influenced by both the bulk (steric *cis* influence) and the σ -donating ability (electronic *trans* influence) of the R groups.^[7] Therefore, the difference, $\delta(\text{Co}–\text{R})$ between the experimental Co–R distances and $d^p(\text{Co}–\text{R})$, is a measure of the contribution of the steric strain to the distance due to the bulk of R, and should correlate with the calculated cone angles of R, $\Theta(\text{R})$. In fact, a good linear relationship is shown in Figure 5a. However, the vertical spread suggests some influence of the bulk of the *trans* N ligand on the Co–R bond, particularly when R is a bulky ligand, although some other secondary effects influencing the Co–C distance should be taken into ac-

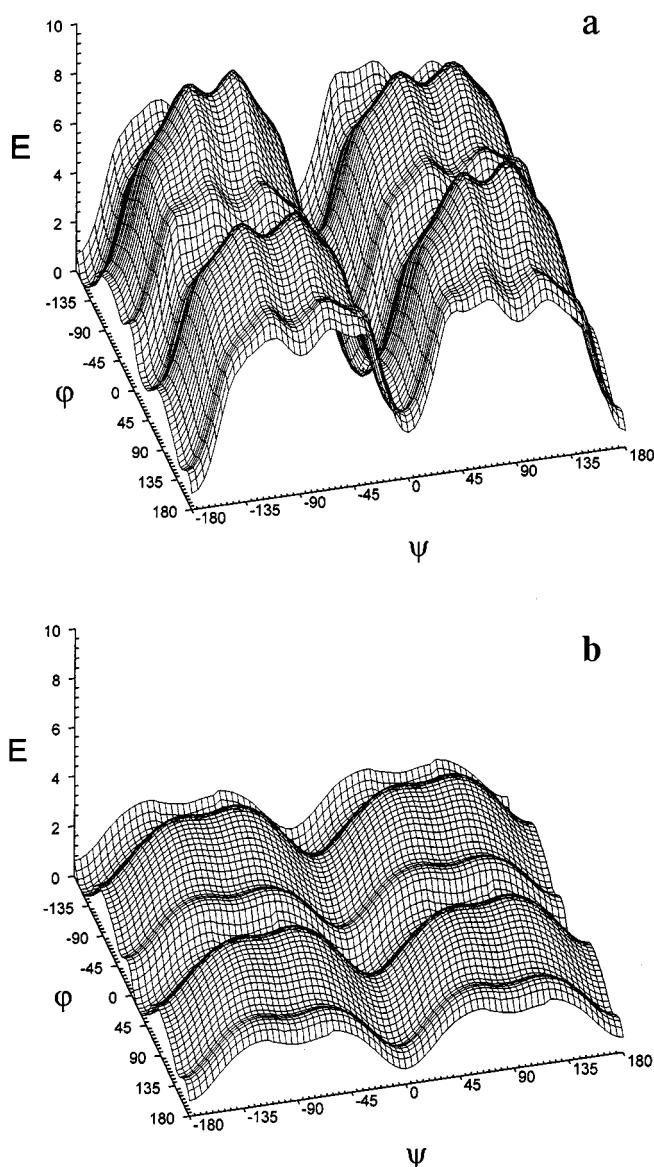


Figure 7. Plot of the strain energy vs. ψ for (ribosyl)Co(DH)₂(1,5,6-Me₃-Bzm) (a) and (ribosyl)Co(DH)₂(Im) (b)

count particularly for lopsided R ligands (*vide infra*). Thus, the calculated Co–adamantyl distances are 2.161 (exp. 2.154) Å and 2.182 (exp. 2.179) Å when L is 1-Me-Im and 1,3,5-Me₃-Bzm, respectively. A more enhanced effect (steric *trans* influence) was observed in adamantylcobaloximes for larger variations in the bulk of L.^[8] In fact, Co–adamantyl distances of 2.129(3) and 2.217(7) Å were found when L = H₂O and PPh₂Et, respectively, whereas for the Me analogues the Co–Me distances were 1.990(5) and 2.026(6) Å, respectively. These results agree with the previous PCA analysis, where the Co–C distances are a linear combination of the three parameters, t_1 , t_2 , and t_3 , whereas the axial Co–N distance is a linear function of only t_1 .^[4b] However, since the t_3 parameter is not easily functionalized, it has not been included in the force field and so the Co–C distance cannot be reproduced well as the Co–N one (Table 3).

Biological Implication

The recent X-ray crystal structure determination of the coenzyme B₁₂ dependent methylmalonyl-CoA mutase^[37] has promoted several studies about the benzimidazole base-off, protein histidine base-on forms of adenosylcobalamin (adoCbl).^[38] In order to make a contribution to the investigation of the role of the cobalt-bound axial bases, we have carried out a conformational analysis on (ribosyl)-Co(DH)₂L complexes with ribosyl = 5-deoxy-β-D-ribofuranos-5-yl and L = 1,5,6-Me₃-Bzm and Im, which are assumed to be acceptable models for the adenosyl base-on benzimidazole and adenosyl base-on histidine species. This allows the study of the geometrical variations induced in the axial fragment upon rotation around the Co–N(ψ) and Co–C(φ) bonds. The three-dimensional plot of the strain energy as a function of ψ and φ for L = 1,5,6-Me₃-Bzm is given in Figure 7a. As expected, it is characterized by steep high potential barriers (ca. 10 kcal mol^{−1}) at ψ ≈ 90° and 270°, over the minima at ψ ≈ 0° and 180°, indicating that the benzimidazole base is restricted by intramolecular forces to an orientation nearly bisecting the oxime bridges. The energy variation with φ is smoother, with a barrier of about 2–3 kcal mol^{−1}. The corresponding plot for L = Im is given in Figure 7b. It is similar to that of Figure 7a, but characterized by significantly lower energy barriers, in spite of the axial Co–N distances, which are on average shorter than those in the benzimidazole case (Table 7). The geometrical parameters of the N–Co–CH₂X fragment, at the highest and lowest energies, are compared in Table 7. This comparison indicates that the conformational strain causes a similar lengthening of the Co–C bonds in the two compounds, but a more marked increase of the Co–N bond length in the benzimidazole derivative. This situation should be even more enhanced when the equatorial ligand is corrin, whose “sentinel” side groups hinder more strongly the rotation around the Co–N axial bond. Thus, it can be concluded that histidine-like bases can rotate about the Co–N bond much more freely than benzimidazole-like ligands, but still significantly stretch the axial Co–N and Co–C bonds. This leads to the suggestion that histidine-like bases can bind to Co more easily than benzimidazole at ψ values which would require axial bond stretchings (vide infra), possibly because of geometrical protein–coenzyme binding demands. These stretchings would contribute both electronically^[1a,39] and sterically^[1b,1c] to enhance the Co–C homolysis, specially after the entrance of the substrate in the active site. It is known that the enhancement of the homolysis rate of about 13 orders of magnitude for adoCbl in the enzyme with respect to the free coenzyme is for 5–6 orders of magnitude attributed to the substrate entrance in the active site.^[40] Inspection of the structural results in the methylmalonyl-coenzymeA mutase^[37] reveals that in addition to the long Co–N(histidine) bond of 2.50 Å, the angles Co–N–C are 130° and 116°. Although of low accuracy, these data indicate that the protein conformation requirements impose on the “symmetric” histidine imidazole an asymmetric coordination to Co (as in lopsided ligands)

with a lengthening of the Co–N bond. The possible consequences upon the Co–C bond stability may be derived from earlier structural and BDE results, obtained for cobaloximes. In fact, comparison of the structures of *i*PrCo(DH)₂Py and *i*PrCo(DH)₂(2-NH₂-py) reveals an abnormally long axial bond of 2.194(4) Å in the latter compared with that of 2.094(2) Å for the py analogue, associated with a strong asymmetry in the Co–N–C angles, which are 115.7(3) and 129.7(4)° (on the side of NH₂).^[12b] These angles are essentially equal and close to 120° in the py derivative. However, only a slight increase of 0.01 Å is observed in the Co–*i*Pr distance in the 2-NH₂-py complex. Correspondingly, Halpern et al.^[12a] have found that the homolytic Co–C BDE in [Ph(Me)CH]Co(DH)₂L is of 17 and 20 kcal mol^{−1} for L = 2-NH₂-py and py, respectively. An opposite trend should be expected from the lower pK_a of the latter ligand (5.2 vs 6.7). If these findings in models, possibly more enhanced, apply to the coenzyme in the active site, it may be concluded that histidine-like ligands are, both sterically and electronically, more suitable than benzimidazole-like ones to respond to the changes induced on the Co coordination geometry favouring homolysis. The fact that substitution of benzimidazole by imidazole gives more thermal Co–C bond heterolysis in cobinamides^[38], a cobalamin-like system, does not contrast with such a hypothesis, since the steric requirements for histidine-like ligands, due to the binding to the protein, are not fulfilled in the free cobinamide. In fact, the two Co–N–C angles are essentially equal to 127° in Co-β-cyanoimidazolylcobamide, but, as well known, they are significantly different in CNCbl (123.3° and 133.0°).^[41] On the other hand, FT Raman spectroscopy measurements in methylcorrinoids^[42] showed that the Co–Me stretching frequency (about 505 cm^{−1}) was only minimally affected by replacement of the benzimidazole by the imidazole moiety. However, these results are obtained in the isolated cobalamin, in which the imidazole is symmetrically coordinated, in contrast to the asymmetric coordination of the histidine within the enzyme.^[37]

Table 7. Coordination bond lengths [Å] and angles [°] for the minimum and maximum energy conformers, of (ribosyl)Co(DH)₂L, with L = Im (ΔE = 4.1 kcal mol^{−1}) and 1,5,6-Me₃-Bzm (ΔE = 9.4 kcal mol^{−1})

	L = Im		L = 1,5,6-Me ₃ -Bzm	
	minimum	maximum	minimum	maximum
Co–N	2.026	2.061	2.068	2.130
Co–C	2.024	2.046	2.031	2.061
Co–C–C	116.5	119.4	116.4	121.1
Co–N–C	127.3	126.9	123.3	121.1
	126.7	127.9	131.0	134.2
N–Co–C	178.1	178.0	179.3	176.4

Conclusion

To our knowledge, this work represents the first example of derivation of a self-consistent force field for organomet-

Table 8. Crystal data and structure refinement for **1** and **2**

	1	2
Empirical formula	C ₁₄ H ₂₁ ClCoN ₅ O ₄	C ₁₃ H ₂₂ ClCoN ₆ O ₄
Formula weight	417.74	420.74
Temperature [K]	293(2)	293(2)
Wavelength [Å]	0.71073	0.71073
Crystal system	triclinic	triclinic
Space group	<i>P</i> −1	<i>P</i> −1
<i>a</i> [Å]	10.569(5)	8.840(1)
<i>b</i> [Å]	13.114(9)	14.629(2)
<i>c</i> [Å]	15.032(7)	14.865(2)
α [°]	108.34(3)	75.04(1)
β [°]	108.01(2)	83.14(1)
γ [°]	96.23(3)	76.58(1)
<i>V</i> [Å ³]	1831(4)	1802.9(5)
<i>Z</i>	4	4
Density (calcd.) [Mg/m ³]	1.516	1.550
Absorption coeff. [mm ^{−1}]	1.11	1.13
<i>F</i> (000)	864	872
Crystal size [mm]	0.2 × 0.3 × 0.3	0.2 × 0.5 × 0.6
θ range for data collection [°]	2 to 28	2 to 26
Index ranges, <i>h k l</i>	−13/13, −17/16, 0/18	−10/10, −17/18, 0/18
Reflections collected	9074	7338
Independent reflections <i>I</i> > 3 σ (<i>I</i>)	4187	4811
<i>R</i> (int)	0.021	0.018
Data/parameters	4187/452	4811/452
Goodness-of-fit on <i>F</i> ²	1.52	1.11
<i>R</i> [<i>I</i> > 3 σ (<i>I</i>)]	0.047	0.034
<i>wR</i> [<i>I</i> > 3 σ (<i>I</i>)]	0.048	0.035
Extinction coeff.	—	2·10 ^{−7}
Largest diff. peak [eÅ ^{−3}]	0.59 and −0.35	0.20 and −0.13

allic complexes which takes into account, in a simple but general way, the electronic *trans* influence.

The present results show that, even if the correlation between the electronic and steric properties of the axial ligands^[4b,43] is neglected, the metal coordination geometry in cobaloximes is well reproduced. The force field could be also applied to the more complex cobalamins, as well as to other vitamin B₁₂ coenzyme models, when MM calculations are used to gain insight into the factors affecting the Co–C cleavage. The present calculations suggest that a change from conformation A to B, stretches essentially the Co–N bond. Since the lengthening of this bond decreases the BDE of the *trans* Co–C bond^[12a] it can be inferred that the Co–C bond is weaker in conformation B. This is supported by near-IR FT-Raman measurements which indicate that in methyl derivatives of similar vitamin B₁₂ models, the Co–Me stretching frequencies (504–506 cm^{−1}) are higher by about 6 cm^{−1} in complexes having an orientation close to A.^[44]

Finally, the conformational analysis, based on the proposed force field, allows the rationalization of the different structural behaviour of the imidazole- and benzimidazole-like ligands in cobaloximes.

Experimental Section

X-ray Diffraction: Compound **1**: C₁₄H₂₁ClCoN₅O₄, *M* = 417.74, triclinic, space group *P* $\bar{1}$, *a* = 10.569(5) Å, *b* = 13.114(9) Å, *c* = 15.032(7) Å, α = 108.34(3)°, β = 108.01(2)°, γ = 96.23(3)°, *V* = 1831(4) Å³, *Z* = 4, *D*_c = 1.516 g/cm³, μ (Mo-*K* α) = 1.11 mm^{−1}, final *R*, *wR*, and *S* are 0.047, 0.048, and 1.52 for 452 parameters

and 4187 unique observed reflections with *I* > 3 σ (*I*). — Compound **2**: C₁₃H₂₂ClCoN₆O₄, *M* = 420.74, triclinic, space group *P* $\bar{1}$, *a* = 8.840(1) Å, *b* = 14.629(2) Å, *c* = 14.865(2) Å, α = 75.04(1)°, β = 83.14(1)°, γ = 76.58(1)°, *V* = 1802.9(5) Å³, *Z* = 4, *D*_c = 1.550 g/cm³, μ (Mo-*K* α) = 1.13 mm^{−1}, final *R*, *wR*, and *S* are 0.034, 0.035, and 1.11 for 452 parameters and 4811 unique observed reflections with *I* > 3 σ (*I*). Data were collected at 293 K using an Enraf Nonius CAD4 single-crystal diffractometer with the Mo-*K* α radiation (λ = 0.71073 Å). The structures were solved by the heavy-atom method. Refinement was carried out by full-matrix least squares of *F*² using the Molen package. Crystallographic data (excluding structure factors) reported in this paper have been deposited at the Cambridge Crystallographic Data Centre and allocated the deposition numbers CCDC-109437 and -109438. Copies of the data can be obtained free of charge on application to CCDC, 12 Union Road, Cambridge CB2 1UZ (Fax: + 44-1223/336-033; E-mail: deposit@ccdc.cam.ac.uk).

Acknowledgments

This work has been supported by the Ministero della Ricerca Scientifica e Tecnologica (Rome) and by the Consiglio Nazionale delle Ricerche (Rome).

[1] [1a] J. Halpern, *Science* **1985**, 227, 869–875. — [1b] N. Bresciani-Pahor, M. Forcolin, L. G. Marzilli, L. Randaccio, M. F. Summers, J. P. Toscano, *Coord. Chem. Rev.* **1985**, 63, 1–125. — [1c] L. Randaccio, N. Bresciani-Pahor, E. Zangrando, L. G. Marzilli, *Chem. Soc. Rev.* **1989**, 18, 225–250.

[2] DH = monoanion of dimethylglyoxime, (DO)(DOH)pn = *N*,*N*'-propanediyilbis(2,3-butanedione 2-imine 3-oxime), salen = dianion of *N,N'*-disalicylidene-ethylenediamine, saloph = dianion of *N,N'*-disalicylidene-*o*-phenylenediamine

[3] [3a] N. Bresciani-Pahor, L. Randaccio, E. Zangrando, *Inorg. Chim. Acta* **1990**, 168, 115–121; P. J. Toscano, H. Brand, S.

- Geremia, L. Randaccio, E. Zangrando, *Organometallics* **1991**, *10*, 713–720 and references therein; C. Tavagnacco, G. Balducci, G. Costa, K. Taschler, W. von Philipsborn, *Helv. Chim. Acta* **1990**, *73*, 1469–1479; A. Sekine, Y. Ohashi, *Bull. Chem. Soc. Jpn.* **1991**, *64*, 2183–2187. — ^[3b] A. Gerli, M. Sabat, L. G. Marzilli, *J. Am. Chem. Soc.* **1992**, *114*, 6711–6718; L. G. Marzilli, A. Gerli, A. M. Calafat, *Inorg. Chem.* **1992**, *31*, 4617–4627; J. P. Charland, E. Zangrando, N. Bresciani-Pahor, L. Randaccio, L. G. Marzilli, *Inorg. Chem.* **1993**, *32*, 4256–4267; R. Dreos, G. Tauzher, S. Vuano, F. Asaro, G. Pelizer, G. Nardin, L. Randaccio, S. Geremia, *J. Organomet. Chem.* **1995**, *505*, 135–138; R. Dreos, G. Tauzher, D. H. Trendafilova, G. Nardin, L. Randaccio, *Inorg. Chem.* **1996**, *35*, 2715–2716; S. M. Polson, L. Hansen, L. G. Marzilli, *Inorg. Chem.* **1997**, *36*, 307–313; S. Geremia, L. Randaccio, E. Zangrando, *Gazz. Chim. Ital.* **1992**, *122*, 229–232.
- [4] ^[4a] E. Zangrando, N. Bresciani-Pahor, L. Randaccio, J. P. Charland, L. G. Marzilli, *Organometallics* **1986**, *5*, 1938–1944. — ^[4b] L. Randaccio, S. Geremia, E. Zangrando, C. Ebert, *Inorg. Chem.* **1994**, *33*, 4641–4650 and references therein. — ^[4c] D. J. A. De Ridder, E. Zangrando, H. B. Burgi, *J. Mol. Struct.* **1996**, *374*, 63–83.
- [5] D. Datta, G. T. Sharma, *J. Chem. Soc. Dalton Trans.* **1989**, 115–118; N. Bresciani-Pahor, S. Geremia, C. Lopez, L. Randaccio, *Inorg. Chem.* **1990**, *29*, 1043–1049; K. L. Brown, S. Satyanarayana, *J. Am. Chem. Soc.* **1992**, *114*, 5674–5684; S. Hirota, S. M. Polson, J. M. Puckett, Jr., S. J. Moore, M. B. Mitchell, L. G. Marzilli, *Inorg. Chem.* **1996**, *35*, 5646–5653 and references therein.
- [6] S. M. Polson, R. Cini, C. Pifferi, L. G. Marzilli, *Inorg. Chem.* **1997**, *36*, 314–322.
- [7] N. Bresciani-Pahor, L. Randaccio, P. J. Toscano, A. C. Sandercock, L. G. Marzilli, *J. Chem. Soc. Dalton Trans.* **1982**, 129–134.
- [8] S. Geremia, L. Randaccio, E. Zangrando, L. Antolini, *J. Organomet. Chem.* **1992**, *425*, 131–139.
- [9] F. T. T. Ng, G. L. Rempel, J. Halpern, *Inorg. Chim. Acta* **1983**, *77*, L165–L166.
- [10] N. Bresciani-Pahor, S. Geremia, E. Zangrando, A. Raeto Raselli, *Inorg. Chim. Acta* **1989**, *162*, 205–209.
- [11] F. T. T. Ng, G. L. Rempel, J. Halpern, *J. Am. Chem. Soc.* **1982**, *104*, 621–623.
- [12] ^[12a] F. T. T. Ng, G. L. Rempel, C. Mancuso, J. Halpern, *Organometallics* **1990**, *9*, 2762–2772. — ^[12b] M. F. Summers, P. J. Toscano, N. Bresciani-Pahor, G. Nardin, L. Randaccio, L. G. Marzilli, *J. Am. Chem. Soc.* **1983**, *105*, 6259–6263.
- [13] L. G. Marzilli in *Bioinorganic Catalysis* (Ed.: J. Reedijk), Marcel Dekker, New York, USA, **1993**, p. 227; C. Krakty, G. Färber, K. Gruber, K. Wilson, Z. Dauter, H. Nolting, R. Konrat, B. Kräutler, *J. Am. Chem. Soc.* **1995**, *117*, 4654–4670.
- [14] J. M. Pratt, *Chem. Soc. Rev.* **1985**, *14*, 161–170; M. K. Geno, J. Halpern, *J. Am. Chem. Soc.* **1987**, *109*, 1238–1239; T. Toraya, A. Ishida, *Biochemistry* **1988**, *27*, 7677–7681; L. G. Marzilli, M. F. Summers, N. Bresciani-Pahor, E. Zangrando, J. P. Charland, L. J. Randaccio, *Am. Chem. Soc.* **1985**, *107*, 6880–6888; L. Randaccio, N. Bresciani-Pahor, E. Zangrando, *Recl. Trav. Chim. Pays-Bas* **1987**, *106*, 343.
- [15] R. D. Hanckock, *Prog. Inorg. Chem.* **1989**, *37*, 187–291.
- [16] B. P. Hay, *Coord. Chem. Rev.* **1993**, *126*, 177–236 and references therein.
- [17] M. Zimmer, *Chem. Rev.* **1995**, *95*, 2629–2649.
- [18] O., Q. Munro, H. M. Marques, P. G. Debrunner, K. Maharao, W. R. Scheidt, *J. Am. Chem. Soc.* **1995**, *117*, 935–954 and references therein.
- [19] ^[19a] H. M. Marques, K. L. Brown, *J. Mol. Struct. (Theochem)* **1995**, *340*, 97–124; H. M. Marques, K. L. Brown, *Polyhedron* **1996**, *15*, 2187–2197. — ^[19b] H. M. Marques, C. Warden, M. Honye, M. S. Shongwe, K. L. Brown, *Inorg. Chem.* **1998**, *37*, 2578–2579. — ^[19c] A. K. Rappé, C. J. Casewit, K. S. Colwell, Goddard, III; W. M. Skiff, *J. Am. Chem. Soc.* **1992**, *114*, 1024–1035; A. K. Rappé, K. S. Colwell, C. J. Casewit, *Inorg. Chem.* **1993**, *32*, 3438–3450.
- [20] P. V. Bernhard, P. Comba, *Inorg. Chem.* **1992**, *31*, 2638–2651.
- [21] M. Calligaris, P. Faleschini, F. Todone, E. Alessio, S. Geremia, *J. Chem. Soc., Dalton Trans.* **1995**, 1653–1661.
- [22] L. M. Hansen, P. N. V. Pavan Kumar, D. S. Marynick, *Inorg. Chem.* **1994**, *33*, 728–735. These calculations confirmed that the steric properties of the R and L ligands, but not their σ -donating ability, influence the Co–C bond. However, this study was limited to alkylcobaloximes without any electron-withdrawing R ligand.
- [23] N. Bresciani-Pahor, L. Randaccio, E. Zangrando, *Inorg. Chim. Acta* **1990**, *168*, 115–121; W. O. Parker, Jr., E. Zangrando, P. A. Marzilli, L. Randaccio, L. G. Marzilli, *Inorg. Chem.* **1988**, *27*, 2170–2180.
- [24] S. Geremia, M. Calligaris, *J. Chem. Soc., Dalton Trans.* **1997**, 1541–1547; S. Geremia, L. Vicentini, M. Calligaris, *Inorg. Chem.* **1998**, *37*, 4094–4103.
- [25] W. D. Cornell, P. Cieplak, I. R. Bayly, I. R. Gould, K. M. J. Merz, D. M. Ferguson, D. C. Spellmeyer, T. Fox, J. W. Caldwell, P. A. Kollman, *J. Am. Chem. Soc.* **1995**, *117*, 5179–5197.
- [26] HYPERCHEM, Hypercube, Inc., Waterloo, Ontario, **1994**.
- [27] R. M. Badger, *J. Chem. Phys.* **1934**, *2*, 128–131.
- [28] D. R. Herschbach, V. W. Laurie, *J. Chem. Phys.* **1961**, *35*, 458–463.
- [29] T. A. Halgren, *J. Mol. Struct. (Theochem.)* **1988**, *163*, 431; *J. Am. Chem. Soc.* **1990**, *112*, 4710–4723.
- [30] O. Ermer, *Struct. Bonding (Berlin)* **1976**, *27*, 161–211.
- [31] P. C. Jurs, *Computer software applications in chemistry*, Wiley, New York, **1996**.
- [32] G. R. Brubaker, D. W. Johnson, *Coord. Chem. Rev.* **1984**, *53*, 1–36.
- [33] A. Immirzi, A. Musco, *Inorg. Chim. Acta* **1977**, *25*, L41–L42.
- [34] A. Bondi, *J. Phys. Chem.* **1964**, *68*, 441–451.
- [35] N. Bresciani-Pahor, W. M. Attia, S. Geremia, L. Randaccio, C. Lopez, *Acta Crystallogr.* **1989**, *C45*, 561–566.
- [36] L. G. Marzilli, M. F. Summers, E. Zangrando, N. Bresciani-Pahor, L. Randaccio, *J. Am. Chem. Soc.* **1986**, *108*, 4830–4838.
- [37] F. Mancia, N. H. Keep, A. Nakagawa, P. F. Leadlay, S. McSweeney, B. Rasmussen, P. Böschke, O. Diat, P. R. Evans, *Structure* **1996**, *4*, 339–350.
- [38] J. M. Sirovatka, R. G. Finke, *J. Am. Chem. Soc.* **1997**, *119*, 3057–3067.
- [39] L. G. Marzilli, M. F. Summers, N. Bresciani-Pahor, E. Zangrando, J. P. Charland, L. Randaccio, *J. Am. Chem. Soc.* **1985**, *107*, 6880–6888; C. Mealli, M. Sabat, L. G. Marzilli, *J. Am. Chem. Soc.* **1987**, *109*, 1593–1594.
- [40] J. M. Pratt, in *Metal Ions in Biological Systems* (Eds.: H. Sigel, A. Sigel), Marcel Dekker, New York, **1993**, p. 229 and references therein.
- [41] B. Kräutler, R. Konrat, E. Stupperich, G. Färber, K. Gruber, C. Kratky, *Inorg. Chem.* **1994**, *33*, 4128–4139. However, it should be noted that in the imidazolylcyanocobalamin, in which an imidazole residue replaces the dimethylbenzimidazole one, the Co–N axial distance is very short [1.978(9) Å].
- [42] J. M. Puckett, Jr., M. B. Mitchell, S. Hirota, L. G. Marzilli, *Inorg. Chem.* **1996**, *35*, 4656–4662.
- [43] S. H. Unger, L. Hausch, *Prog. Phys. Org. Chem.* **1976**, *12*, 91.
- [44] S. Hirota, S. M. Polson, J. M. Puckett, Jr., S. J. Moore, M. B. Mitchell, L. G. Marzilli, *Inorg. Chem.* **1996**, *35*, 5646–5653.

Received November 19, 1998
[I98399]